Received: 19 December 2017 | Accepted: 3 April 2018

DOI: 10.1002/jbio.201700386

Journal of BIOPHOTONICS

FULL ARTICLE

Label-free bacterial colony detection and viability assessment by continuous-wave terahertz transmission imaging

Xiang Yang[1] | Jia Shi[2,3] | Yuye Wang[2,3]* | Ke Yang[1] | Xiang Zhao[1] | Guiyu Wang[1] | Degang Xu[2,3] | Yunxia Wang[1] | Jianquan Yao[2,3] | Weiling Fu[1]*

[1]Department of Laboratory Medicine, Southwest Hospital, Third Military Medical University (Army Medical University), Chongqing, China

[2]Institute of Laser and Optoelectronics, School of Precision Instrument and Optoelectronic Engineering, Tianjin University, Tianjin, China

[3]Key Laboratory of Optoelectronic Information Science and Technology (Ministry of Education), Tianjin University, Tianjin, China

***Correspondence**

Yuye Wang, Institute of Laser and Optoelectronics, School of Precision Instrument and Optoelectronic Engineering, Tianjin University, Tianjin 300072, China.
Email: yuyewang@tju.edu.cn

Weiling Fu, Department of Laboratory Medicine, Southwest Hospital, Third Military Medical University (Army Medical University), Chongqing 400038, China.
Email: weiling_fu@126.com

Funding information

The National Basic Research Program of China, Grant/Award Number: 2015CB755400; the National Natural Science Foundation of China, Grant/Award Number: 81430054; China Postdoctoral Science Foundation, Grant/Award Number: 2016M602954; the Basic Science and Frontier Technology Research Project of Chong Qing, Grant/Award Number: cstc2017jcyjBX0004; Postdoctoral Science Foundation of Chongqing, Grant/Award Number: Xm2016021; the Joint Incubation Project of Southwest Hospital, Grant/Award Number: SWH2016LHJC04, SWH2016LHJC01

Timely and accurate bacterial detection is critical for various health and safety applications, which promotes the continuous development of versatile optical sensors for bacterial investigations. Here, we report a new strategy for bacterial colony sensing using terahertz (THz) imaging with minimal assay procedures. The proposed method utilizes the acute sensitivity of THz wave to the changes in the water content and cellular structures. Single bacterial colonies of 4 bacterial species were directly distinguished using THz imaging by utilizing their differences in THz absorption. In addition, the distribution of mixed bacterial samples has been demonstrated by THz imaging, which demonstrated that the target bacterium could be easily recognized. Furthermore, we investigated the differentiation of bacterial viability, which indicated that bacteria under different living states could be distinguished by THz imaging because of their different hydration levels and cellular structures. Our results suggest that THz imaging has the potential to be used for mixed bacterial sample detection and bacterial viability assessment in a label-free and nondestructive manner.

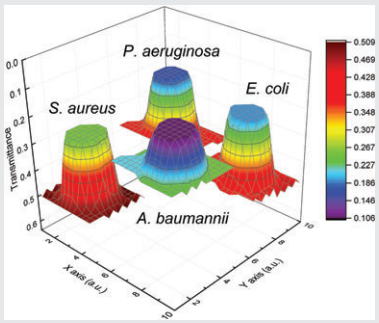

KEYWORDS

bacterial detection, biosensor, terahertz imaging, THz absorption

1 | INTRODUCTION

The rapid detection of bacterial species and their living states is of great importance in many fields, including the food industry and clinical medicine. For instance, the detection of dead bacteria in patient specimens is not significant for making a clinical diagnosis [1], because the potential hazards are limited to the living portion of mixed bacterial populations [2]. Matrix-assisted laser desorption ionization-time-of-flight mass spectrometry (MALDI-TOF MS) and nucleic acid amplification tests (NAATs) have facilitated dramatic advances in bacterial detection. However, in most cases, these methods cannot be used to distinguish between living and dead species; instead, they only confirm the presence of target proteins or nucleic acids, respectively. On the other hand, most routine methods for distinguishing between

Xiang Yang and Jia Shi contributed equally to this study.

living and dead bacteria use DNA-binding dyes to evaluate the membrane integrity. Samples are unavoidably destroyed by the added reagents, hindering further confirmatory tests or subsequent experimental assays [3]. Therefore, a rapid and simple method is urgently needed for identifying bacteria and evaluating their viability in a label-free manner.

The terahertz (THz) region of the electromagnetic spectrum is typically defined as 0.1 to 10 THz. The energy levels of weak interactions, including hydrogen bonds and van der Waals forces, coincidently lie within the THz range; thus, water is notoriously highly absorbent of THz wave [4, 5]. By utilizing this contrast mechanism, various healthy, tumor, dehydrated and burned tissues could be clearly differentiated by THz spectroscopy and imaging according to their different hydration levels [6, 7]. Researchers have demonstrated that THz spectroscopy has a greater sensitivity for detecting subtle structural changes of cells than conventional optical phase contrast microscopy [8]. As a result, THz technology has been extensively applied in various biomedical applications, such as probing hydration dynamics [9], detecting DNA hybridization [10], investigating cytoplasm leakage in real time [11], imaging cancer tissues [12] and detecting bacteria [13]. Specifically, some THz signatures (absorption peaks) have been found for spores of *bacillus* species [14–16], complementing Raman and infrared spectral signatures for bacterial spore identification. Different types of bacterial colonies could also be differentiated by THz spectroscopy because of their different water contents, although no obvious signatures were found at room temperature as a result of the complexity of vegetative cellular components [17, 18]. In addition, living and dead bacteria also exhibited different THz absorption because of the different hydration levels and structural characteristics [19]. Therefore, THz spectroscopy has proven to be a label-free alternative in bacterial detection and viability evaluation.

However, the studies described above focused only on investigating pure bacterial colonies using THz spectroscopy. In practical applications, the rapid detection of the composition and distribution of mixed bacterial samples is also important. For instance, several bacterial colonies may overlap on a culture medium if the parent cells are too close together. This is particularly true when detecting mixed or polymicrobial specimens. The prompt detection of the mixed samples and recognition of the portion of interest would be helpful for more accurately targeting bacterium identification in a short amount of time. Additionally, relatively large numbers of samples were required in the previous spectroscopic study [17], hindering its practical applications in the food industry or clinical laboratories. Consequently, there is an increasing interest in using THz imaging for detecting the distributions of different bacterial colonies, particularly mixed bacterial colonies. Notwithstanding such potential, 2 issues need to be addressed when applying THz imaging to bacterial detection. First, rapid detection speeds are favorable for timely bacterial identification and reduce the effects of the experimental environment and sample changes. In conventional THz time-domain spectroscopy (THz-TDS), scanning speeds are relatively slow because of the time delay scanning. Additionally, THz-TDS has difficulty in detecting high-moisture products as a result of the relatively low output power [20]. Second, the sizes of bacterial colonies on a blood agar medium are typically only 1 to 4 mm in size (depending on the species); thus, higher THz frequencies are preferable for obtaining a higher image resolution.

In this study, we used a continuous-wave THz imaging system in transmission mode to investigate the characteristics of single bacterial colonies and the distributions of mixed bacterial colonies, to demonstrate its practical usage for bacterial colony sensing. Single bacterial colonies of *Escherichia coli*, *Staphylococcus aureus*, *Acinetobacter baumannii* and *Pseudomonas aeruginosa* were effectively differentiated by THz imaging from their different THz absorption. Using this contrast mechanism, the distributions of the mixed samples were clearly demonstrated, and the target bacterium was easily recognized. In addition, living and dead bacteria were successfully distinguished based on their different hydration levels and structural characteristics. Moreover, living bacteria in the sample cell were monitored continuously using THz imaging within 3 hours, demonstrating the potential of the method for the label-free assessment of bacterial viability.

2 | MATERIALS AND METHODS

2.1 | Bacterial sample preparation

Standard bacterial strains (*E. coli* ATCC 25922, *S. aureus* ATCC 25923, *A. baumannii* ATCC 19606 and *P. aeruginosa* ATCC 27853) were obtained from the National Institute for the Control of Pharmaceutical and Biological Products, China. After activation from −80°C, the bacteria were inoculated overnight on Columbia blood agar medium (CNA, Pang tong, Chongqing, China) at 37°C in an atmosphere containing 5% CO_2. Then, bacterial colonies were scraped off the surface of the solid medium for direct measurement. Dead bacteria were prepared by treating the bacterial colonies in Eppendorf tubes in a metal bath at 100°C for 60 minutes. The Eppendorf tubes were sealed with Parafilm to minimize evaporative water losses during thermal treatment. Then, the samples were evenly mixed and cooled to room temperature before removing the Parafilm for measurement.

2.2 | Continuous-wave THz imaging system

A continuous-wave THz imaging system in transmission mode was used to detect bacterial samples, as depicted in Figure 1A. The source was an optically pumped continuous-wave THz gas laser (FIRL100, Edinburgh Instruments Ltd, UK). The THz frequency was fixed at 2.52 THz with an output power of 40 mW. Golay cells (GC-1P, Tydex Ltd, Russia)

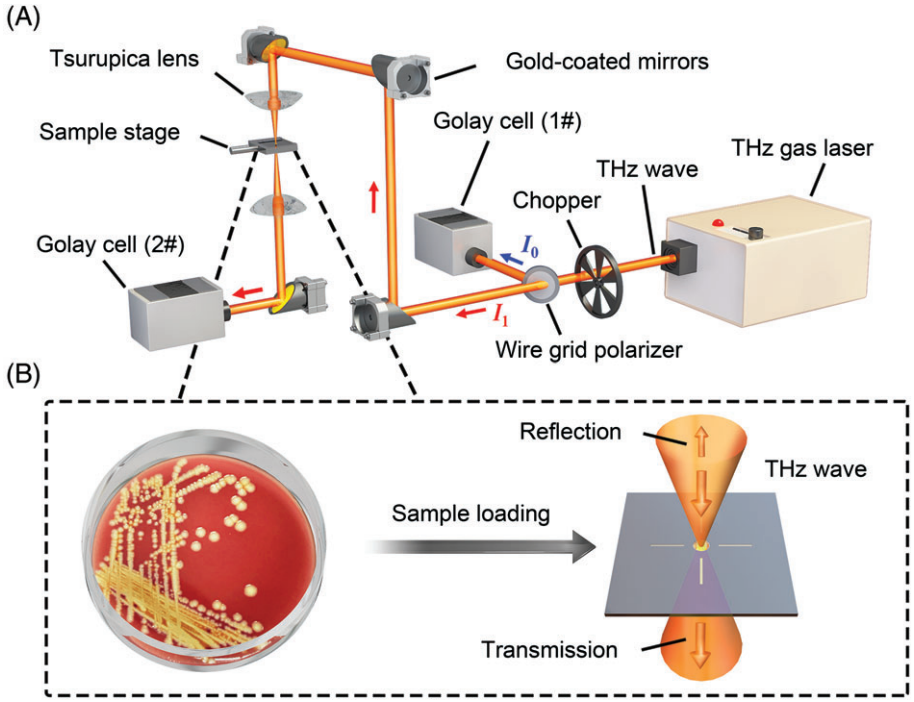

FIGURE 1 Bacterial colony detection by THz imaging. (A) Schematic of the continuous-wave THz transmission imaging system. (B) Schematic of sample loading and THz measurement

were used as the detectors and operated at room temperature. Considering the responsivity of the detectors, the THz wave output was modulated as a sinusoidal signal using a chopper operating at 50 Hz. In order to reduce the image noises due to slight power fluctuations, THz wave was separated into transmitted and reflected beams as the signal (I_1) and reference (I_0) by a wire grid polarizer. The reference beam was detected by a Golay cell (#1). Meanwhile, the signal beam was focused on the sample with a confocal system consisting of 2 Tsurupica lenses ($f = 30$ mm) and detected by a Golay cell (#2). The sample was placed on a computer-controlled horizontal *x*-*y* scanning stage, and 2-dimensional image (P) can be obtained with the pixel value of I_1/I_0. The resolution of this imaging system was 260 × 380 μm (measured by the knife-edge method), and the scanning step was fixed at 100 μm in this study.

For every measurement, we employed a sample cell composed of a sample plate and cover quartz plate. The sample plate, which was made of a silicon wafer (thickness = 300 μm, resistivity >10 kΩ·cm), was fabricated using conventional photolithography technology (Karl Suss MA6, Suss MicroTec, München, Germany). Then, a central cavity surrounded by 4 indicator lines was created in the sample plate. The cavity was 2 mm in diameter and 20 μm in depth, and the volume of the cavity was approximately 0.06 μL, allowing single bacterial colonies to be detected.

2.3 | Measurement protocol

After culture, a portion of an isolated colony was spotted into the central cavity for direct measurement, as shown in Figure 1B. The sample plate was covered with a quartz plate, and excessive bacteria cells were poured out of the cavity to ensure that it was completely filled. Then, the sample cell was placed on the *x*-*y* stage for THz imaging. After measurement, the sample cavity was treated to reduce bacterial adhesion with 1 mL of a trypsin solution for 3 minutes at room temperature, followed by a rinsing with distilled water. To minimize the influence of experimental conditions, every species of bacteria was observed in 5 samples, and 3 independent experiments were conducted on different days. Hence, 15 samples of each species of bacteria were measured to minimize sample heterogeneity. Bacteria were inoculated and handled safely in a Level II biosafety cabinet.

2.4 | Data analysis

Considering that both the quartz and silicon plates have high transmittances in the THz band of interest, the reflected THz intensity caused by the marginal Fresnel loss due to their different refractive indices can be neglected during scanning. The sample cell with and without bacteria were measured as the images of P_{sample} and $P_{\text{substrate}}$, respectively. Owing to the uniformity of sample cell and the small depth of sample cavity, the averaged value V_{bac} for the pixels in sample cavity of $P_{\text{substrate}}$ was taken as the image reference for simplicity. Thus, the distribution of sample transmittance can be calculated by dividing the pixel values in P_{sample} by V_{bac}. Similarly, the transmittance of sample cell is obtained by using the air as the reference. The averaged transmittance, T_{ave}, is defined as the average of multiple pixels within the regions of interest. Statistical analyses were conducted by calculating the values of T_{ave} and the standard deviations of the 15 individual data values in each group. A Kruskal-Wallis test was used to compare the imaging results for different bacterial species, followed by a Dunn's multiple

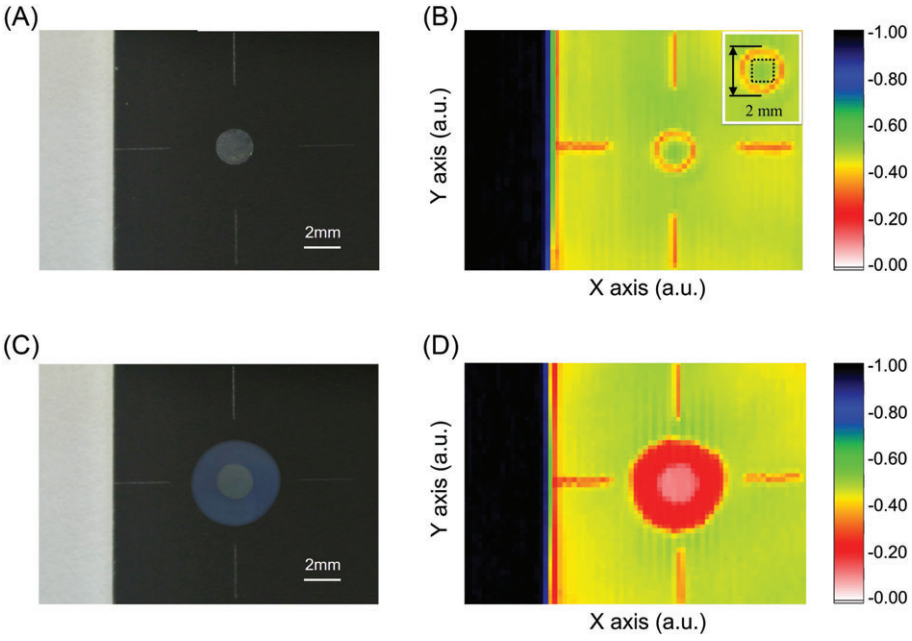

FIGURE 2 THz imaging of the sample cell before and after adding bacterial colony. (A) Visible image of the empty sample cell. (B) Transmittance of the empty sample cell. (C) Visible image of the sample cell after adding *Staphylococcus aureus.* (D) Transmittance of the sample cell after adding *S. aureus*

comparison test. An additional independent *t* test was used to test for a significant difference between living and dead bacteria. All analyses were conducted using the statistical software SPSS software 20.0; a *P* value of <.05 was considered to be statistically significant.

3 | RESULTS

3.1 | THz imaging of different bacterial colonies

To demonstrate the uniformity of the sample cell and the reliability of the measurement protocol, we measured the sample cell without and with bacteria. Figure 2A,C shows the visible images of the sample cell before and after adding *S. aureus* bacteria, respectively. It is noted that the air area beside the sample cell was chosen and simultaneously imaged, which is completely transparent in the THz range. Correspondingly, Figure 2B,D shows the transmittances of the sample cell before and after adding *S. aureus*, where the air area was used as the reference. The transmittance of air areas was 100%, corresponding to the black areas in Figure 2B,D. The transmittances of the cavity area without bacteria and its surrounding area were similar, indicating the uniformity of the sample cell. Moreover, when the quartz cover plate was bonded onto the sample plate through the middle bacterial layer, excess bacteria cells spilled out of the central cavity. Accordingly, the pink areas in Figure 2D indicate the sample in the cavity, and the red areas represent overflowing bacterial cells. We can see that the bacteria were well-distributed in the cavity using our preparation method. Three other bacteria species were measured in the same way.

For a quantitative comparison, the transmittances of bacterial colonies were used in the following analysis, where the reference was calculated from $P_{substrate}$ by averaging the data obtained in a selected area of the sample cavity (denoted by the black dashed rectangle in the inset of Figure 2B). Figure 3 shows the stereogram imaging results from drawing the sample transmittances on the *z* axis. The top surface of the cylinder represents the transmittance distribution of the detected bacteria in the cavity, while the bottom surface represents the overflowing bacterial cells. The top surfaces of the central cylinders were quite flat, indicating that the cavities were fully and evenly filled with samples. The transmittance of the overflowing layer was much higher than that of the cells in the cavity, demonstrating that the depth of overflowing bacterial cells was considerably shallower compared to that of the cells in the cavity. The 4 species of bacteria had different surface colors. *A. baumannii* exhibited the highest THz absorption among the 4 species, while *S. aureus* exhibited the lowest absorption. According to their different surfaces, *P. aeruginosa* was more absorbing than *E. coli.* The results can be explained by the differing water contents of the 4 species, which agrees with the previous spectroscopic investigation [17]. Figure 3B presents a comparison of T_{ave} for the 4 bacterial species: 10.8% ± 1.3% for *A. baumannii*, 16.2% ± 1.3% for *P. aeruginosa*, 18.7% ± 1.2% for *E. coli* and 24.6% ± 2.1% for *S. aureus.* By conducting nonparametric Kruskal-Wallis tests followed by Dunn's multiple comparison tests, statistically significant differences were observed between all pairings of different bacteria ($P < .05$).

3.2 | THz imaging of mixed bacterial samples

After illustrating the differences in the imaging results between bacterial species, we explored the THz imaging analysis of mixed bacterial samples. Considering that *P. aeruginosa* can be preliminarily identified by its

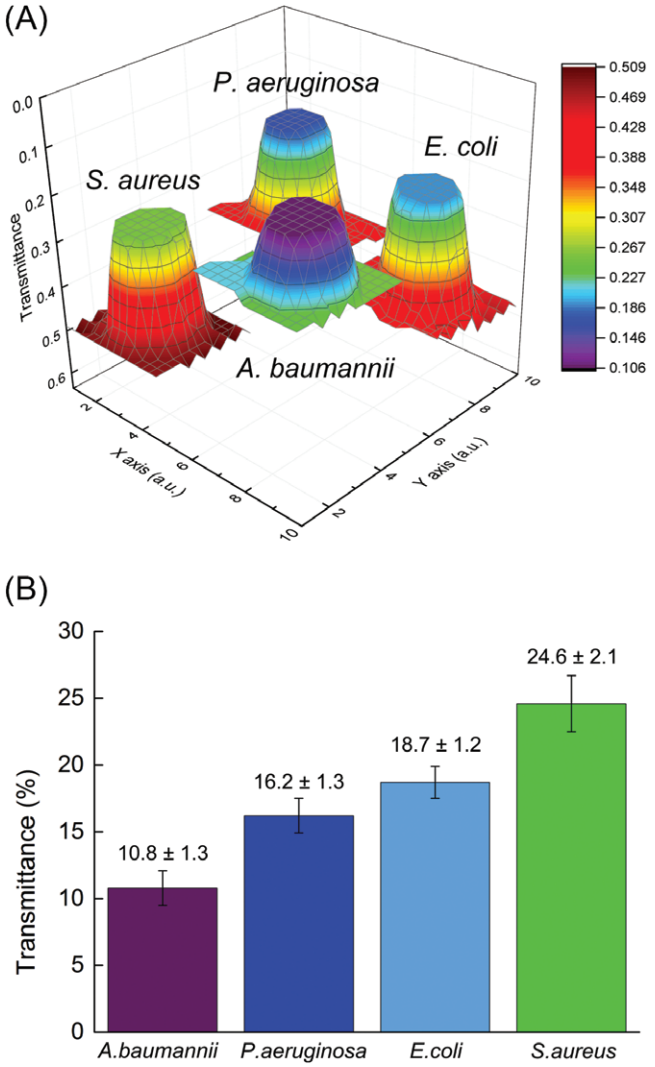

FIGURE 3 THz imaging of different bacterial colonies. (A) Comparison of THz images for different bacteria in stereo view. Note that 4 independent tests for different bacteria were drawn in the same coordinate system for easy comparison. (B) Statistical analysis of the average transmittances of 4 bacterial groups after multiple measurements ($n = 15$). Data are shown as mean ± SD. The differences between each pair of groups were evaluated using the Kruskal-Wallis method followed by a Dunn's multiple comparison test ($P < .05$)

characteristic odor[21] and *S. aureus* can be preliminarily identified by its typical hemolytic zones on blood agar plates [22], mixed bacterial samples composed of *E. coli* and *A. baumannii* were investigated. To mimic the overlapping bacterial colonies on an agar medium, different amounts of the 2 bacteria were spotted onto opposite sides of the inner edge of the central cavity. When the sample plate was covered with the quartz plate, bacteria were squeezed inside to form a mixed sample. Figure 4A shows a THz image of the sample mixed at a proportion of 5:5. The result demonstrated that the 2 bacterial colonies, which are difficult to discern with the naked eye, could be effectively recognized using THz imaging. The obvious boundary between the purple and light blue colors clearly delineates the sample distribution inside the central cavity. *A. baumannii* samples, which have stronger liquidity because of their higher water content, tended to occupy more space than *E. coli* samples during the squeezing. More precisely, the surface colors were identical to those of pure samples (Figure 3A) for the same color bar scale. The inherent THz absorption properties of bacteria in mixed samples can still be effectively displayed by THz imaging, allowing for easy and direct recognition of a target bacterium in mixed samples. In addition, an obvious boundary between the purple and light blue colors was also observed in Figure 4B with a proportion of 7:3. This result demonstrated that the 2 bacterial colonies mixed at different proportions could be effectively distinguished. However, the boundary was not very clear in Figure 4C when the mixing proportion increased to 9:1. The small amount of *E. coli* in the bacterial colonies was not able to be effectively recognized using THz imaging, which could be attributed to the resolution limit of the imaging system.

3.3 | THz imaging for bacterial viability assessment

In addition to using THz imaging to identify different bacterial species, we used THz imaging to assess bacterial viability. Figure 5 shows a comparison of THz imaging results for living and dead *S. aureus*; obvious THz absorption differences can be observed for the 2 states. According to an independent *t* test, the 2 groups exhibited statistically significant differences (24.6% ± 2.1% vs 30.0% ± 2.3% for living and dead *S. aureus*, respectively; $P < .05$). This can be explained by differences in both cellular structures and water content. The structural variability of bacterial cells, such as

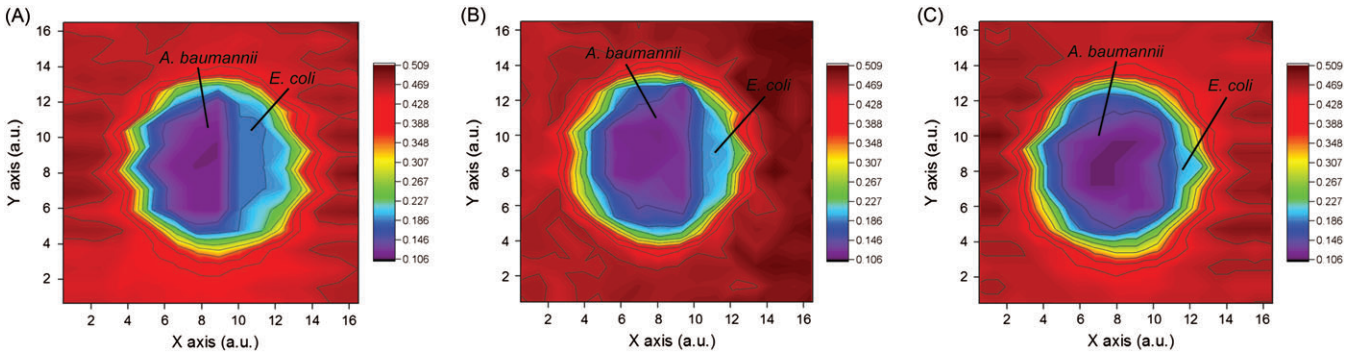

FIGURE 4 THz imaging of *Acinetobacter baumannii* and *Escherichia coli* samples mixed at different proportions. (A) 5:5 mixing. (B) 7:3 mixing. (C) 9:1 mixing

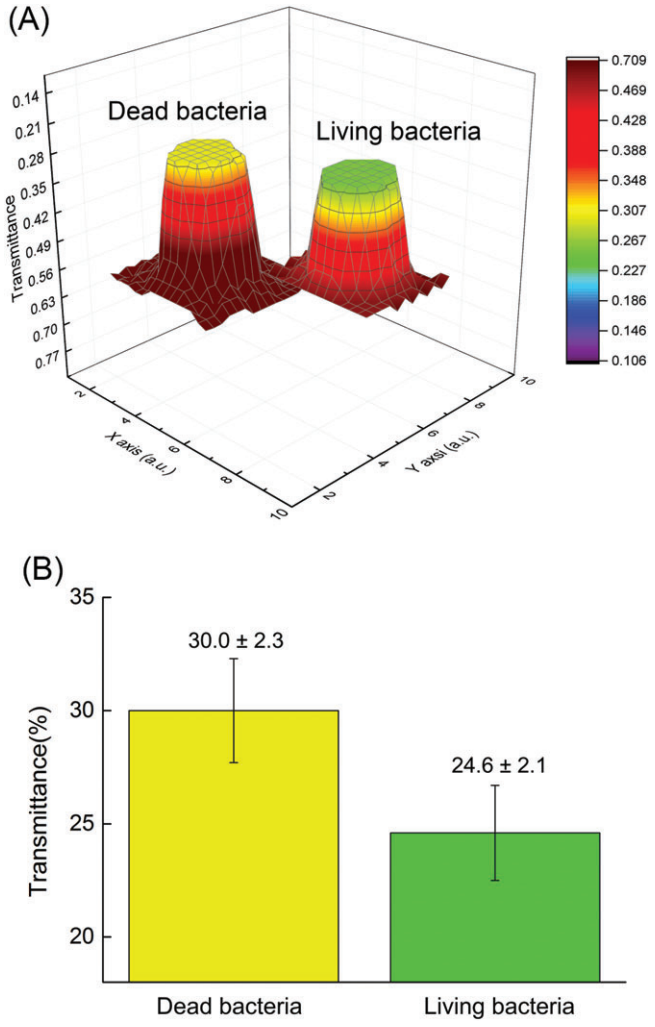

FIGURE 5 THz imaging of living and dead bacteria. (A) Comparison of THz images of living and dead *Staphylococcus aureus*. Note that 2 independent tests were drawn in the same coordinate system for easy comparison. (B) Statistical analysis of the average transmittances of 2 groups after multiple measurements ($n = 15$). Data are shown as mean ± SD. An independent t test was used to statistically compare the 2 groups ($P < .05$)

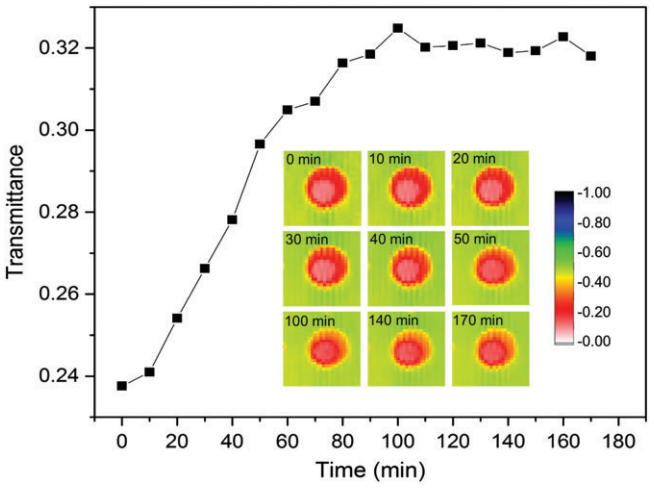

FIGURE 6 Viability monitoring of *Staphylococcus aureus* by THz imaging for 3 hours at 10-minute intervals. The insets show representative results at different time points

protein denaturation, during thermal treatment led to changes in low-frequency biomolecular motions, including molecular vibration and rotation [23]. As a result, bacterial viability can be effectively displayed by THz imaging because these low-frequency vibration modes coincidently lie in the THz frequency range. Based on this principle, recent work demonstrated the feasibility of using THz imaging to quantitatively measure the permeability of epithelial cells [11]. In addition, the change in water content should be a more important factor for their different THz responses. Hydration water (ie, the intracellular water molecules in the immediate vicinity of biomolecular surfaces) exhibits a different THz response than the surrounding bulk water [9, 24]. Because water molecules are closely associated with metabolic activities [25], the changes in water content (especially the hydration-water-to-bulk-water ratios) should be responsible for the significant THz absorption differences between living and dead *S. aureus*. A similar investigation demonstrated that THz spectral differences between *Bacillus thuringiensis* samples in the log phase and late stationary phase could be attributed to the tiny changes in hydration levels [15], which is in agreement with our results.

To investigate the changes in bacterial viability after bacteria were removed from the culture medium, we monitored the same sample with THz imaging for 3 hours at 10-minute intervals. Figure 6 shows the changes in the average THz transmittances of living *S. aureus* after being spotted into the sample cell. The THz transmittance increased gradually for the first 100 minutes and then remained at an approximately constant level (~32%). As shown in the insets, no significant changes were observed inside the cavities (pink areas) in the first 40 minutes. After 40 minutes, the samples in the cavity became uneven, and the overflowing samples (red areas) become smaller. The increased THz transmittance for these 40 minutes may be attributable to the reduced metabolic activity of the bacteria after leaving the culture medium (in particular, the changes in intracellular hydration states) [26]. Meanwhile, the accumulated metabolic wastes in bacterial cells in the spacer might also be responsible for this phenomenon. The exact mechanisms have not yet been discovered because of the complexity of intracellular components. After 40 minutes, we observed obvious sample shrinkage due to cell dehydration and water evaporation. Hence, the transmittance of the uneven samples in the cavity increased to an even higher level, and became comparable to that of dead *S. aureus*. Therefore, the measurement results were affected by both the: (1) viability changes that occurred after bacteria left the culture medium and (2) inevitable shrinkage of the sample over time. Accordingly, a standardized operation procedure including the detection time should be a necessary prerequisite for acquiring accurate bacterial species identification results. Instead of replacing routine use in clinical laboratories, THz imaging would be more useful

for continuous bacterial monitoring, such as detecting intracellular metabolites in high-throughput industrial strain screening processes [27], by utilizing its high sensitivity to the hydration levels and structural changes.

4 | DISCUSSION

Our results have demonstrated the applicability of THz imaging to detect 4 bacterial species and mixed bacterial samples. The results indicated that gram-negative bacteria (*E. coli, A. baumannii and P. aeruginosa*) tended to absorb more THz wave than gram-positive bacteria (*S. aureus*). This phenomenon was also observed in a previous spectroscopic study of additional species [28]. It remains unclear whether this trend is biased by the limited number of tested species; further investigation of other species would be worthwhile. As with other optical sensors [29], the presence of the target bacteria can be quickly and directly identified from color changes in THz imaging, without the need for further analytical assays. Hence, THz imaging could be very useful in cases where medically important bacteria must be promptly identified before appropriate actions can be taken (eg, when *Bacillus anthracis* must be unambiguously identified). Similar to the spectral profiles for MALDI-TOF MS, identifying an unknown bacterium requires establishing a THz database containing the target bacteria of interest under same culture conditions. In addition, living and dead bacteria possessed different THz responses, hinting at novel strategies for assessing bacterial viability in a label-free manner. Accordingly, THz imaging may lay a foundation for developing a new antimicrobial susceptibility test by monitoring tested bacteria subject to particular antibiotics.

In conventional bacterial detection methods, laborious assay procedures are required for metabolic and phenotypic analyses [30]. Considering that the reagent cost per identification is approximately $2.5 to 5.0 [31], THz imaging offers another tantalizing possibility for label-free and reagentless bacterial detection. Similar to other biophysical properties of bacterial colonies, such as the forward-scattering patterns produced by light-scattering technologies [3, 32], the THz responses of bacterial colonies can be directly utilized for bacterial detection within 10 minutes after culture. Compared with other mainstream bacterial detection methods [13], THz imaging has several advantages, as summarized in Table 1. In particular, MALDI-TOF MS can only detect isolated pure colonies after culture due to its limitation in separating multiple spectra collected simultaneously [1]. Therefore, THz imaging would be helpful for pre-analyzing mixed colonies on a solid medium, which is favorable for detecting mixed or polymicrobial specimens. Unlike dye-based molecular methods, THz imaging enables the label-free investigation of bacterial viability. In this noncontact and nondestructive method, the sample remains intact during the analysis of its biophysical properties, which would be useful when further confirmatory tests or subsequent experimental assays are required.

There are still some challenges facing the widespread application of THz imaging for bacterial detection. First, THz imaging has a poor sensitivity because of the size mismatch between THz radiation and bacterial cells. The wavelength of THz wave at 1 THz is approximately 300 μm, while a single bacterial cell has a typical diameter of 1 to 3 μm. Accordingly, relatively large numbers of samples are generally required for detection. In addition, the spatial resolution is limited by the diffraction of THz wave. Although post-culture bacterial colonies are large enough to be detected, near-field THz techniques with a greatly improved spatial resolution are preferable for the detection of small amounts of bacteria. Second, the operating performance of THz systems should be further improved for practical applications. For instance, a better sensitivity for detecting small amounts of bacteria requires the use of more sensitive detectors such as Schottky diode mixers [33]. Compact THz sources with a high output power may serve as promising substitutes for developing miniaturization systems. Additionally, rapid sampling methods such as compressed sensing [34] are worthy for attempting to realize bacterial imaging with accelerated imaging speeds. All of these improvements are deemed essential before THz imaging can be applied in the food industry or medical laboratories.

TABLE 1 Characteristics of bacterial detection by THz imaging compared with common methods

Characteristic	THz imaging	Traditional culture methods	MALDI-TOF MS	NAATs
Detection principle	THz absorption differences between bacteria	Metabolic and phenotypic analysis	Spectra based on protein mass-to-charge ratios	Specific nucleic acid amplification
Time for bacterial detection	Minutes after culture	Days to weeks	Minutes after culture	One to several hours
Simplicity	Yes	No	Yes	No
Reagentless detection	Yes	No	Yes (only matrix is needed)	No
Living/dead bacteria discrimination	Yes	No	No	No (except reverse transcriptase polymerase chain reaction)
Mixed bacterial sample analysis	Yes	Yes	No	Yes
Limit of detection	0.06 μL (the sensitivity in this study)	-	10^5-10^6 cfu	Several to tens of genome equivalents

5 | CONCLUSIONS

In summary, we used a continuous-wave THz imaging system for bacterial detection with minimal sample preparation. To the best of our knowledge, this is the first study using THz imaging to differentiate between bacterial species and to determine bacterial viability. Utilizing the biophysical properties of bacterial colonies, a fast, simple, cost-effective and 1-step method for analyzing bacterial colonies was proposed. It would be worthwhile to further investigate the selectivity between more or less virulent strains of same bacteria; this might require better instrument performance and standard operating procedures. Because of the high sensitivity of THz wave to the water content and bacterial cell structures, certain future applications can be envisioned, such as the continuous monitoring of fermentation processes. Although our current methodology still needs significant improvements, particularly in terms of the detection sensitivity, our results provide a proof-of-concept demonstration that THz imaging could be developed into an alternative approach for bacterial analysis that is label-free, reagentless and nondestructive.

ACKNOWLEDGMENTS

This work was supported by the National Basic Research Program of China (2015CB755400), the National Natural Science Foundation of China (81430054), the China Postdoctoral Science Foundation (2016M602954), the Basic Science and Frontier Technology Research Project of Chong Qing (cstc2017jcyjBX0004), the Postdoctoral Science Foundation of Chongqing (Xm2016021) and the Joint Incubation Project of Southwest Hospital (SWH2016LHJC04 and SWH2016LHJC01).

ORCID

Weiling Fu http://orcid.org/0000-0002-2695-6604

REFERENCES

[1] B. W. Buchan, N. A. Ledeboer, *Clin. Microbiol. Rev.* **2014**, *27*, 783.
[2] A. Nocker, C.-Y. Cheung, A. K. Camper, *J. Microbiol. Methods.* **2006**, *67*, 310.
[3] P. P. Banada, K. Huff, E. Bae, B. Rajwa, A. Aroonnual, B. Bayraktar, A. Adil, J. P. Robinson, E. D. Hirleman, A. K. Bhunia, *Biosens Bioelectron.* **2009**, *24*, 1685.
[4] E. Pickwell, V. P. Wallace, *J. Phys. D Appl. Phys.* **2006**, *39*, R301.
[5] J.-H. Son, *Nanotechnology* **2013**, *24*, 214001.
[6] G. J. Wilmink, B. L. Ibey, T. Thomas, S. Brian, L. Norman, X. G. Peralta, C. C. Roth, C. Z. Cerna, B. D. Rivest, J. E. Grundt, *J. Biomed. Opt.* **2011**, *16*, 047006.
[7] P. Tewari, C. P. Kealey, D. B. Bennett, N. Bajwa, K. S. Barnett, R. S. Singh, M. O. Culjat, A. Stojadinovic, W. S. Grundfest, Z. D. Taylor, *J. Biomed. Opt.* **2012**, *17*, 040503.
[8] H.-B. Liu, G. Plopper, S. Earley, Y. Chen, B. Ferguson, X. C. Zhang, *Biosens Bioelectron.* **2007**, *22*, 1075.
[9] B. Born, S. J. Kim, S. Ebbinghaus, M. Gruebele, M. Havenith, *Faraday Discuss.* **2009**, *141*, 161.
[10] M. I. Lvovska, N. C. Seeman, R. Sha, T. R. Globus, T. B. Khromova, T. S. Dorofeeva, *IEEE Trans. Nanotechnol.* **2010**, *9*, 610.
[11] M. Grognot, G. Gallot, *Appl. Phys. Lett.* **2015**, *107*, 103702.
[12] S. J. Oh, S.-H. Kim, Y. B. Ji, K. Jeong, Y. Park, J. Yang, D. W. Park, S. K. Noh, S.-G. Kang, Y.-M. Huh, J.-H. Son, J.-S. Suh, *Biomed. Opt. Express* **2014**, *5*, 2837.
[13] X. Yang, K. Yang, Y. Luo, W. Fu, *Appl. Microbiol. Biotechnol.* **2016**, *100*, 5289.
[14] E. R. Brown, T. B. Khromova, T. Globus, D. L. Woolard, J. O. Jensen, A. Majewski, *IEEE Sensors J.* **2006**, *6*, 1076.
[15] W. Zhang, E. R. Brown, L. Viveros, K. P. Burris, C. N. Stewart Jr., *J. Biophotonics.* **2014**, *7*, 818.
[16] E. R. Brown, J. E. Bjarnason, T. L. J. Chan, A. W. M. Lee, M. A. Celis, *Appl. Phys. Lett.* **2004**, *84*, 3438.
[17] X. Yang, D. Wei, S. Yan, Y. Liu, S. Yu, M. Zhang, Z. Yang, X. Zhu, Q. Huang, H.-L. Cui, W. Fu, *J. Biophotonics.* **2016**, *9*, 1050.
[18] T. Globus, A. M. Moyer, B. Gelmont, T. Khromova, M. I. Lvovska, I. Sizov, J. Ferrance, *IEEE Sensors J.* **2013**, *13*, 72.
[19] T. Globus, T. Dorofeeva, I. Sizov, B. Gelmont, M. Lvovska, T. Khromova, O. Chertihin, Y. Koryakina, *Am. J. Biomed. Eng.* **2012**, *2*, 143.
[20] K. Wang, D.-W. Sun, H. Pu, *Trends Food Sci. Technol.* **2017**, *67*, 93.
[21] E. O. King, M. K. Ward, D. E. Raney, *J. Lab. Clin. Med.* **1954**, *44*, 301.
[22] Y. Persson, A.-K. J. Nyman, U. Gronlund-Andersson, *Acta Vet. Scand.* **2011**, *53*, 36.
[23] X. Yang, X. Zhao, K. Yang, Y. Liu, Y. Liu, W. Fu, Y. Luo, *Trends Biotechnol.* **2016**, *34*, 810.
[24] K. Shiraga, T. Suzuki, N. Kondo, K. Tanaka, Y. Ogawa, *Appl. Phys. Lett.* **2015**, *106*, 253701.
[25] R. Cooke, I. D. Kuntz, *Ann. Rev. Biophys. Bioeng.* **1974**, *3*, 95.
[26] K. Shiraga, Y. Ogawa, T. Suzuki, N. Kondo, A. Irisawa, M. Imamura, *J. Infrared Millim. Te.* **2014**, *35*, 493.
[27] C. Wang, J. Gong, Q. Xing, Y. Li, F. Liu, X. Zhao, L. Chai, C. Wang, A. M. Zheltikov, *J. Biophotonics* **2010**, *3*, 641.
[28] A. Berrier, M. C. Schaafsma, G. Nonglaton, J. Bergquist, J. G. Rivas, *Biomed. Opt. Express* **2012**, *3*, 2937.
[29] S. M. Yoo, S. Y. Lee, *Trends Biotechnol.* **2016**, *34*, 7.
[30] A. E. Clark, E. J. Kaleta, A. Arora, D. M. Wolk, *Clin. Microbiol. Rev.* **2013**, *26*, 547.
[31] A. M. Caliendo, D. N. Gilbert, C. C. Ginocchio, K. E. Hanson, L. May, T. C. Quinn, F. C. Tenover, D. Alland, A. J. Blaschke, R. A. Bonomo, K. C. Carroll, M. J. Ferraro, L. R. Hirschhorn, W. P. Joseph, T. Karchmer, A. T. MacIntyre, L. B. Reller, A. F. Jackson, *Clin. Infect. Dis.* **2013**, *57*, S139.
[32] P. P. Banada, S. Guo, B. Bayraktar, E. Bae, B. Rajwa, J. P. Robinson, E. D. Hirleman, A. K. Bhunia, *Biosens Bioelectron.* **2007**, *22*, 1664.
[33] A. Maestrini, B. Thomas, H. Wang, C. Jung, J. Treuttel, Y. Jin, G. Chattopadhyay, I. Mehdi, G. Beaudin, *C. R. Phys.* **2010**, *11*, 480.
[34] K. Kim, D. G. Lee, W. G. Ham, J. Ku, S. H. Lee, C. B. Ahn, J. H. Son, H. Park, *IEEE Trans. THz Sci. Technol.* **2013**, *3*, 395.

How to cite this article: Yang X, Shi J, Wang Y, et al. Label-free bacterial colony detection and viability assessment by continuous-wave terahertz transmission imaging. *J. Biophotonics*. 2018;11:e201700386. https://doi.org/10.1002/jbio.201700386